Current Research in Toxicology 6 (2024) 100161

Contents lists available at ScienceDirect

Current Research in Toxicology

journal homepage: www.journals.elsevier.com/current-research-in-toxicology

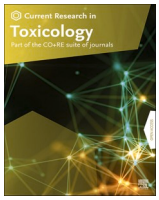

Cigarette smoking inhibits myoblast regeneration by promoting proteasomal degradation of NPAT protein and hindering cell cycle progression

Jianfeng Wang [a,1], Jinling Liu [b,1], Jingjing Shao [a], Hongyu Chen [c,d], Luyun Cui [a], Pei Zhang [a], Yinan Yao [a], Jianying Zhou [a,*], Zhang Bao [a,*]

[a] Department of Pulmonary and Critical Care Medicine, The First Affiliated Hospital, Zhejiang University School of Medicine, Hangzhou 310003, China
[b] Department of Pulmonology, the Children's Hospital, Zhejiang University School of Medicine, National Clinical Research Center for Child Health, Hangzhou 310058 China
[c] School of Medicine, Hangzhou City University, Hangzhou 310015, China
[d] Institute of Bioinformatics and James D. Watson Institute of Genome Sciences, Zhejiang University, Hangzhou 310058, China

ARTICLE INFO

Keywords:
Cigarette smoking
Myoblast proliferation
Cell cycle
NPAT
Proteasome

ABSTRACT

Cigarette smoking (CS) causes skeletal muscle dysfunction, leading to sarcopenia and worse prognosis of patients with diverse systemic diseases. Here, we found that CS exposure prevented C2C12 myoblasts proliferation in a dose-dependent manner. Immunoblotting assays verified that CS exposure promoted the expression of cell cycle suppressor protein p21. Furthermore, CS exposure significantly inhibited replication-dependent (RD) histone transcription and caused S phase arrest in the cell cycle during C2C12 proliferation. Mechanistically, CS deregulated the expression levels of Nuclear Protein Ataxia-Telangiectasia Locus (NPAT/p220). Notably, the proteasome inhibitor MG132 was able to reverse the expression of NPAT in myoblasts, implying that the degradation of CS-mediated NPAT is proteasome-dependent. Overexpression of NPAT also rescued the defective proliferation phenotype induced by CS in C2C12 myoblasts. Taken together, we suggest that CS exposure induces NPAT degradation in C2C12 myoblasts and impairs myogenic proliferation through NPAT associated proteasomal-dependent mechanisms. As an application of the proteasome inhibitor MG132 or overexpression of NPAT could reverse the impaired proliferation of myoblasts induced by CS, the recovery of myoblast proliferation may be potential strategies to treat CS-related skeletal muscle dysfunction.

1. Introduction

Cigarette smoking (CS) can cause respiratory diseases, such as lung cancer, chronic obstructive pulmonary disease (COPD), and respiratory failure, through various mechanisms such as inflammation and oxidative stress (Christenson et al., 2022; Morse and Rosas, 2014; Stampfli and Anderson, 2009). Among these diseases, COPD is a common chronic lung disease characterized by persistent airflow limitation, and CS is one of the main causes (Agusti et al., 2023). Sarcopenia is a common comorbidity of COPD characterized by decreased skeletal muscle mass and strength, with a risk of physical disability, reduced quality of life, and death. COPD patients with sarcopenia have a poor prognosis and high mortality (Christenson et al., 2022). However, the cause of CS induced sarcopenia is not well understood yet. Several studies have identified CS as a risk factor for sarcopenia. In the MINOS cohort study of 845 men aged 45–85, smokers had lower relative appendicular skeletal muscle mass than those who had never smoked, demonstrating that cigarette smoking is a risk factor for sarcopenia (Szulc et al., 2004). Furthermore, a Rancho Bernardo cohort study, which examined the prevalence and risk factors of sarcopenia in 694 men and 1,006 women aged 55–98,

Abbreviations: CS, cigarette smoking; CHX, Cycloheximide; COPD, chronic obstructive pulmonary diseases; DMEM, Dulbecco's Modified Eagle Medium; DMSO, dimethyl sulfoxide; DNA, deoxyribonucleic acid; FBS, fetal bovine serum; FITC, fluorescein isothiocyanate; GM, growth medium; Hsp, heat shock protein; OD, optical density; qRT-PCR, quantitative real-time reverse-transcription polymerase chain reaction; RD, replication-dependent; RNA, Ribonucleic Acid; NPAT, Protein Ataxia-Telangiectasia Locus; HiNF-P, Histone Nuclear Factor P; CDK, Cyclin-dependent kinase; HLB, histone locus body; SEM, standard error of mean.

* Corresponding authors.
E-mail addresses: zjyhz@zju.edu.cn (J. Zhou), baozhang@zju.edi.cn (Z. Bao).

[1] Jianfeng Wang and Jinling Liu contributed equally to this work.

https://doi.org/10.1016/j.crtox.2024.100161
Received 15 July 2023; Received in revised form 16 February 2024; Accepted 1 March 2024
Available online 2 March 2024

identified cigarette smoking as a reversible risk factor for sarcopenia (Castillo et al., 2003). Moreover, a similar work demonstrated that sarcopenia in community-dwelling older Chinese men and women was associated with CS (Lee et al., 2007). However, the cellular and molecular mechanisms leading to CS-associated muscle breakdown remain elusive. Nonetheless, recent studies have shed some clues that may explain the mechanisms underlying CS-induced muscle protein degradation (Kim et al., 2011; Lee et al., 2021).

The maintenance of skeletal muscle mass is related to the metabolism of skeletal muscle cells and the regenerative ability of skeletal muscle stem cells (satellite cells) (Cong et al., 2020; Dumont et al., 2015; Hood et al., 2019; Kaczmarek et al., 2021). The research on COPD complicated with sarcopenia has focused on the metabolism of skeletal muscle cells and the direction of skeletal muscle atrophy and senescence (Hood et al., 2019; Ito et al., 2022), but there is few research on the regeneration of skeletal muscle satellite cells. Studies have shown that a reduction in the number and activity of satellite cells is an important cause of skeletal muscle loss (Zhang et al., 2018). The mechanism by which CS regulates the regenerative capacity of skeletal muscle satellite cells has not been well explained.

During eukaryotic cell proliferation, replication-dependent (RD) histone proteins must be synthesized concurrently with DNA duplication to replicate chromosomes in the S phase (Mendiratta et al., 2019). Synthesis of RD histone mRNA occurs in a specific nuclear body called the histone locus body (HLB), which is tethered to histone gene clusters. The HLB is a dynamic structure that forms in stem cells just after mitosis (Duronio and Marzluff, 2017a; Mao et al., 2011; Nizami et al., 2010a; Sleeman and Trinkle-Mulcahy, 2014). Nuclear Protein Ataxia-Telangiectasia Locus (NPAT/p220) is a key regulator for HLB formation, acting as a foundation for the initiation of protein–protein interaction-based HLB assembly (Becker et al., 2010; Ye et al., 2003; Zheng et al., 2015). As a commonly used marker to distinguish HLB structure from other nuclear compartments, NPAT is essential for the self-renewal of stem cells and is confirmed to be indispensable in both Drosophila and murine development (Nizami et al., 2010b; Wright et al., 2017). Thus, NPAT activation must be fine-tuned for the accurate regulation of proliferation and development. However, it is unclear whether the regulation of NPAT protein is stimulated by external factors such as CS exposure.

In the present study, we investigated the effects and molecular mechanisms of CS on the proliferation of C2C12 myoblasts. CS could inhibit the cell proliferation by inhibiting RD histone transcription and causing S phase arrest in the cell cycle. CS significantly decreased the expression levels of NPAT, which is essential for RD histone transcription. Moreover, we found that CS inhibited myoblast regeneration by promoting the proteasomal degradation of NPAT protein. Notably, we confirmed that CS inhibited the expression of HiNF-P, which has been demonstrated to stabilize the NPAT (Miele et al., 2005). The proteasome inhibitor MG132 was able to reverse CS-induced degradation of NPAT and S phase arrest during the cell cycle in C2C12 myoblast. This study sheds light on the molecular mechanisms of CS toxicity and presents a potential rationale for mitigating tobacco-induced sarcopenia.

2. Methods

2.1. Cell culture and transfection

C2C12 myoblasts (Cell Bank of the Chinese Academy of Science, China) were grown in DMEM (high glucose) supplemented with 15 % (v/v) fetal bovine serum (FBS), 100 U/mL penicillin, and 100 mg/mL streptomycin (Hyclone Laboratories, Logan, UT, USA). The cells were transfected with lipofectamine 2000 (Invitrogen, Fish Scientific, Carlsbad, CA, USA) according to the protocol of the manufacturer (Cong et al., 2020; Wang et al., 2004).

2.2. Construction of expression plasmids

Full-length cDNA of NPAT were cloned into a hemagglutinin FLAG-tagged expression vector, pXJ40 (Dr E Manser, IMCB, Singapore). To confirm their identity, several clones were chosen and sequenced in both directions for each construct by professional sequencing facility (Shangya Biotechnology Co., LTD, Zhejiang, China). All plasmids were purified using an Axygen miniprep kit (Axygen, Tewksburg, MA, USA) for use in transfection experiments. The Escherichia coli strain DH5 (Invitrogen) was used as a host for propagation of the clones.

2.3. CS exposure

3R4F reference cigarettes (University of Kentucky, Lexington, KY, USA) were selected for CS exposure experiments. All cigarettes were conditioned at 22 °C ± 1 °C and 60 % ± 3 % relative humidity for at least 48 h before being used in the experiments.

Cell exposure treatment was based on the *in vitro* air–liquid interface model. For CS exposure treatment experiments, the cells were seeded onto Transwell inserts (Corning Incorporated, USA) with a 3-μm polycarbonate membrane at a density of 2.0×10^4 cells/cm^2. Thereafter, an air–liquid interface was established by removing the medium from the apical surface and exposing only the basal surface of the cells to the medium. The cells were further used for subsequent air and CS exposures by Borgwaldt RM20S (Borgwaldt KC GmbH, Hamburg, Germany), which is a rotary syringe smoking machine specifically designed for *in vitro* biological toxicity assessment of CS. The whole CS was diluted with laboratory air (Temperature 22 °C ± 1 °C; Humidity 60 % ± 3 %) to series times (50×, 300 ×) to expose C2C12 cells maintained at the air–liquid interface in exposure chambers housed at 37 °C for 2 h. The puffing regimen was set according to the International Organization for Standardization (ISO3308:2012) with the following parameters: a 35-ml puff drawn over 2 s every 1 min period; a 5 min cycle per cigarette yielding 12 cigarettes smoked per 1 h of treatment. To avoid potential exposure to CS components in the nutrient solution due to aerosol sedimentation, a peristaltic pump was used to replace the nutrient solution at a flow rate of 3 ml/min. Cells were collected for further experiments. (Sup. Fig. 1).

2.4. Immunoblotting

Cells were lysed in lysis buffer (150 mM sodium chloride, 50 mM Tris, pH 7.3, 0.25 mM EDTA, 1 % [wt/vol] sodium deoxycholate, 1 % [vol/vol] Triton X-100, 0.2 % sodium fluoride, 0.1 % sodium orthovanadate, and a mixture of protease inhibitors from Roche Applied Science, Indianapolis, IN). Lysates were then analyzed by immunoblotting for the indicated antibodies. Anti-NPAT [A302-771A] was obtained from Bethyl (Montgomery, TX, USA). Anti- HiNF-P [sc-373855] and anti-p21 [sc-53870] were obtained from Santa Cruz Biotechnology (Dallas, TX, USA). Anti- Phe, phospho (Ser/Thr) [9631S] was obtained from Cell Signaling Technology (Danvers, MA, USA). Anti-tubulin [M1305-2] and anti-actin [M1210-2] were obtained from HuaAn Biotechnology (Hangzhou, China).

2.5. Immunofluorescence

The cells were seeded on coverslips in a six-well plate for 24 h. Cells in chamber slides were fixed with 3 % formaldehyde in PBS at 4 °C for 20 min and permeabilized with 0.5 % Triton buffer (0.5 % Triton X-100, 20 mM HEPES-KOH [pH 7.4], 50 mM NaCl, 3 mM MgCl) for 10 min at room temperature. After being blocking with 10 % bovine serum albumin (BSA) in PBS for 1 h, cells were treated with a primary Ab overnight. P21 and NPAT proteins were detected using anti-p21 (sc-53870, Santa Cruz Biotechnology) and anti-NPAT (A302-771A, Bethyl) followed by Alexa Fluor 488-conjugated goat anti-mouse IgG or anti-rabbit IgG (Invitrogen). The cells were then observed using confocal fluorescence

microscopy for immunofluorescence detection. The images were collected using a 63 × 1.4NA or 20 × objective lens through appropriate laser excitation on an LSM510 Meta laser-scanning confocal microscope (Carl Zeiss) or an Olympus IX81-FV1000 laser-scanning confocal microscope. The images were analyzed using Zeiss LSM Image Examiner Software or FV10-ASW 3.0 Viewer.

2.6. Quantitative real-time reverse-transcription polymerase chain reaction (qRT-PCR)

Total RNA was extracted using the RNeasy Kit (Qiagen, Chatsworth, CA, USA). Reverse transcription was performed using a SuperScript III reverse transcriptase kit (Invitrogen). cDNA was quantified using the KAPA SYBR FAST qPCR MasterMix Kit (Kapa Biosystems, Wilmington, MA, USA) and a real-time PCR system (Applied Biosystems, Foster City, CA, USA). The primer sets for qRT-PCR are:

-Primer: H2A Forward: CGTGCTGGAGTACCTGACG
- Primer: H2A Reverse: CTTGTTGAGCTCCTCGTCGT
- Primer: H2B Forward: AGCTGGTGTACTTGGTGACG
- Primer: H2B Reverse: TACAACAAGCGCTCGACCAT
- Primer: H3 Forward: CGTGGGTCTGTTTGAGGACA
- Primer: H3 Reverse: TGTCCTTGGGCATGATGGTG
- Primer: H4 Forward: ATGTCTGGTCGTGGCAAGG
- Primer: H4 Reverse: TGTTGTCACGCAGCACTTTG
- Primer: Actin Forward: ATGCTCCCCGGGCTGTAT
- Primer: Actin Reverse: ATGCTCCCCGGGCTGTAT
- Primer: p53 Forward: GGCGTAAACGCTTCGAGATG
- Primer: p53 Reverse: CTTCAGGTAGCTGGAGTGAGC
- Primer: p27 Forward: TCAAACGTGAGAGTGTCTAACG
- Primer: p27 Reverse: CCGGGCCGAAGAGATTTCTG
- Primer: p16 Forward: CGTACCCCGATTCAGGTGAT
- Primer: p16 Reverse: TTGAGCAGAAGAGCTGCTACGT

2.7. Chemical reagents

Cycloheximide (CHX) was obtained from Abcam (CAS 66–81-9, Cambridge, UK) and dissolved in DMSO (to a final concentration of below 0.1 %). The proteasome inhibitor (MG132) was obtained from Santa Cruz (sc-201270) and dissolved in DMSO (to a final concentration of below 0.1 %).

2.8. Cycloheximide (CHX) chase assay

For the CHX chase assay, C2C12 cells were treated with CHX (50 μg/mL) and harvested at the indicated time points (0, 3, 6, 9, 12, and 15 h after treatment). The treated cells were lysed, and the lysates were then analyzed using immunoblotting with anti-NPAT and anti-tubulin antibodies.

2.9. Proteasome inhibitor MG132 rescue assay

For the MG132 rescue assay, C2C12 cells were treated with MG132 (4 μg/mL) for 12 h before harvesting. The treated cells were lysed and, the lysates were analyzed using immunoblotting with anti-NPAT and anti-tubulin antibodies.

2.10. Cell proliferation assays

In this experiment, we established two dilution concentration gradients of 3R4F smoke: the ratio of CS and air were 1:300 and 1:50. C2C12 cells were cultured in the proliferation medium containing air and 3R4F smoke for 2 h and then CS exposure was stopped. Then cells were plated at a density of 200/100-mmdiameter culture dis. Cells were incubated for 10 days, and the medium was replaced on alternate days. Colonies were visualized with methylene blue and prior to quantification.

2.11. Cell counting Kit-8 (CCK8) assay

The effect of CS on cell viability was assessed by Cell Counting Kit-8 (CCK8) assay (HY-K0301, MedChemExpress, NJ, USA). 10 μl of CCK8 reagent was added to each well and the cells were incubated for 2 h at 37 °C. The optical density (OD) at 450 nm was measured by using SynergyMx M5 (Molecular Devices, CA, USA).

2.12. Flow cytometry

For flow cytometry, cells were harvested, fixed in ethanol, and stained with propidium iodide. Flow cytometry analysis was performed with a FACS can instrument (Ling Zheng et al., 2015).

2.13. Statistical analysis

The data are recorded as means ± SEM. For comparison between two groups, if the data fitted a normal distribution, a two-tailed unpaired Student's *t*-test was used when variances were similar by F test ($p > 0.05$). Whereas a two-tailed unpaired Student's *t*-test with Welch's correction was used when variances were different by F test ($p < 0.05$). If the data did not fit a normal distribution, a Mann-Whitney *U* test was used. If the variation among three or more groups was minimal, ANOVA followed by Dunnett's post-test or Tukey's post hoc test was applied for comparison of multiple groups. Statistical significance was determined as indicated in the figure legends. *$p < 0.05$, **$p < 0.01$, ***$p < 0.001$. The GraphPad Prism 9 software (La Jolla, CA, USA) was used for analysis.

3. Results

3.1. Smoke exposure inhibits the proliferation of C2C12 cells

To explore the effect of smoke exposure on the proliferation of C2C12 cell, we established two dilution concentration gradients of 3R4F smoke: the ratio of CS and air were 1:300 and 1:50. The proliferation ability of C2C12 cells was reflected by the number of cell clones (Fig. 1A and B). The results demonstrated that compared with the control group without smoke, the number of clones in the smoke treatment group decreased significantly, and the number of clones decreased with the increase in smoke concentration. Similarly, the CCK-8 experiment revealed that the OD value of the smoke treatment group decreased compared with the control group, and the OD value decreased more obviously with the increase in smoke concentration (Fig. 1C). These results suggested that CS exposure inhibited the proliferation of C2C12 cells in a concentration-dependent manner.

3.2. The inhibitory effects of CS on the proliferation of C2C12 cells depends on the up-regulation of p21 expression

An appropriate control over cell cycle progression depends on many factors. Cyclin-dependent kinase (CDK) inhibitor p21 (also known as p21(WAF1/Cip1)) is one of these factors that promote cell cycle arrest in response to a variety of stimuli(Karimian et al., 2016). We found that smoke treatment could up-regulate the expression of p21 compared with the control group without smoke (Fig. 2A). Moreover, immunofluorescence results also revealed that smoking exposure could promote the expression of p21 compared with the control group (Fig. 2B). These findings suggest that smoking can inhibit the proliferation of C2C12 cells by up-regulating the expression of p21. Moreover, further qPCR experiments demonstrated that CS exposure could also obviously increase the mRNA expression of p53, which was upstream of p21and mildly increase the mRNA expression of other cell cycle suppressors, such as p27and p16. (Fig. 2C).

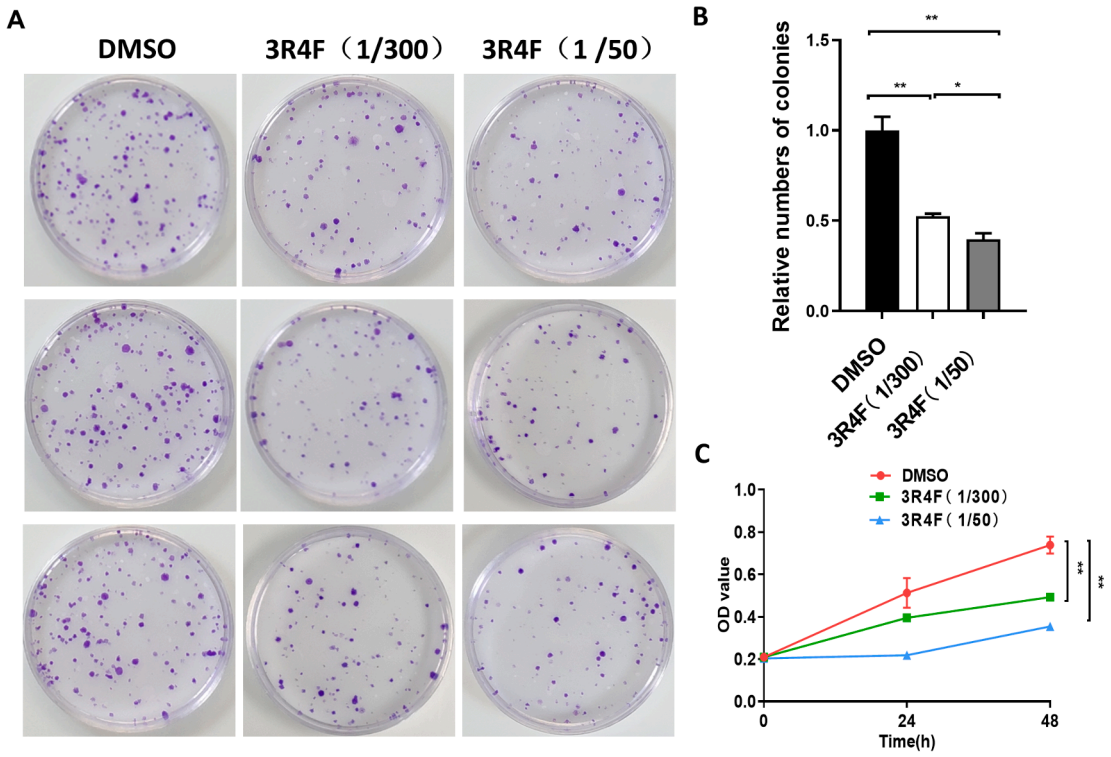

Fig. 1. CS treatment inhibited myoblasts proliferation. (A) Colony formation was performed on C2C12 myoblasts with air and air-CS mixture (the ratio of CS and air was 1:300 or 1:50) treatment. (B) Relative numbers of colonies were analyzed. N = 3. ANOVA followed by Dunnett's post-test was applied for comparison. Significant difference from control, *p < 0.05, **p < 0.01. (C) CCK8 assay was performed on C2C12 myoblasts with or without CS (the ratio of CS and air was 1:300 or 1:50) treatment. Quantification analysis for OD value was performed. N = 3. ANOVA followed by Dunnett's post-test was applied for comparison. Significant difference from control, **p < 0.01.

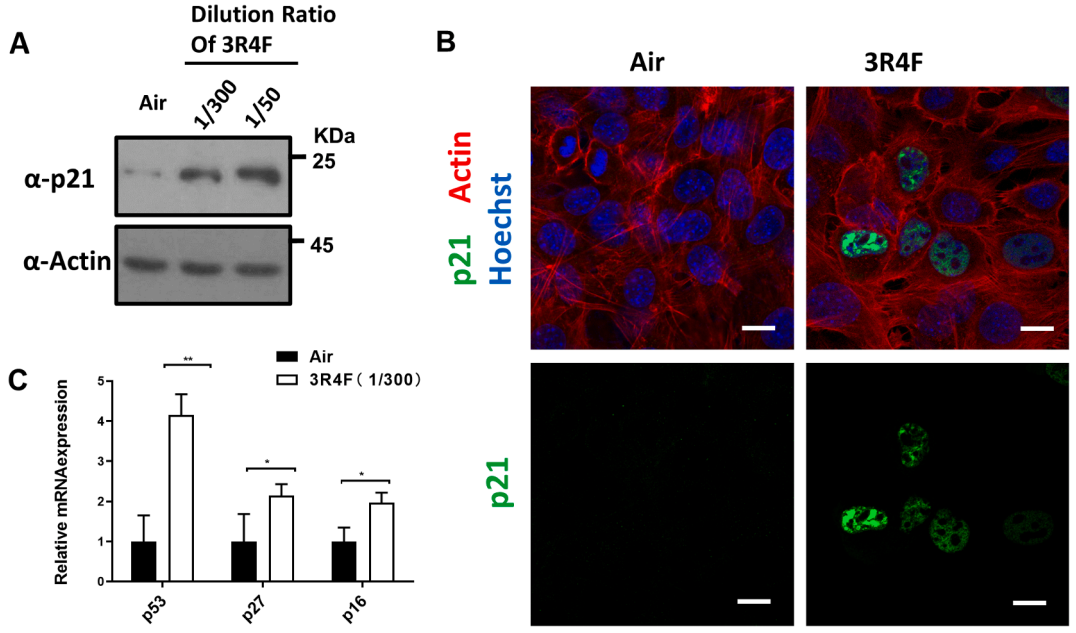

Fig. 2. CS treatment increased the expression of p21. (A) Lysates of C2C12 myoblasts treated with air and air-CS mixture (the ratio of CS and air was 1:300 or 1:50) were western blotted with p21 antibody. Actin antibody was used as the loading control. (B) C2C12 myoblasts were treated with air and air-CS mixture (the ratio of CS and air was 1:300). Cell morphology of the myoblasts was examined through immunofluorescence. P21 (green) was detected through direct staining with its antibody. Nuclei (blue) were visualized through Hoechst staining. (C) Total mRNA of C2C12 myoblasts treated with air and air-CS mixture (the ratio of CS and air was 1:300) was extracted, and the gene expression of p27, p16 and p53 was detected using real-time PCR. Tubulin was used as an internal control. Values are shown as means ± SEM. N = 3. A two-tailed unpaired Student's *t*-test was used. Significant difference from control, *p < 0.05. **p < 0.01. (For interpretation of the references to colour in this figure legend, the reader is referred to the web version of this article.)

3.3. CS exposure caused S phase arrest during the myoblast cell cycle by decreasing the expression of NPAT protein

We calculated the proportion of myoblasts in different stages during the cell cycle exposed to CS through flow cytometry. We found that the proportion of cells increased in the S phase after smoke treatment compared with the control group, which indicated that CS exposure caused S phase arrest (Fig. 3A). We also found that 3R4F standard smoke exposure significantly inhibited replication-dependent histone transcription in myoblasts compared with the air exposure group (Fig. 3B). These findings suggest that smoke exposure may promote the withdrawal of the cell cycle by inhibiting histone transcription, thus down-regulating the proliferation ability of myoblasts. We further compared the expression of NPAT protein in myoblasts exposed to different concentrations of CS. We found that CS exposure could inhibit the expression of NPAT protein in myoblasts in a concentration-dependent manner (Fig. 3C). Moreover, we found that CS exposure inhibited both the expression of NPAT protein and its phosphorylation regulation (Fig. 3D). During cell proliferation, NPAT protein is expressed mostly in the nucleus of proliferating cells as punctate aggregates (Ye et al., 2003). Our experiments demonstrated that CS exposure could significantly inhibit the expression of NPAT protein in myoblasts, and the higher the smoke concentration, the fewer NPAT spots in the nucleus (Fig. 3E). However, CS exposure did not affect the mRNA transcription level of NPAT in myoblasts, even at higher concentrations of smoke exposure (Fig. 3F). To sum up, our experiments demonstrated that CS exposure inhibited S-phase entry during the myoblast cell cycle by down-regulating the expression of NPAT protein but not its transcription level.

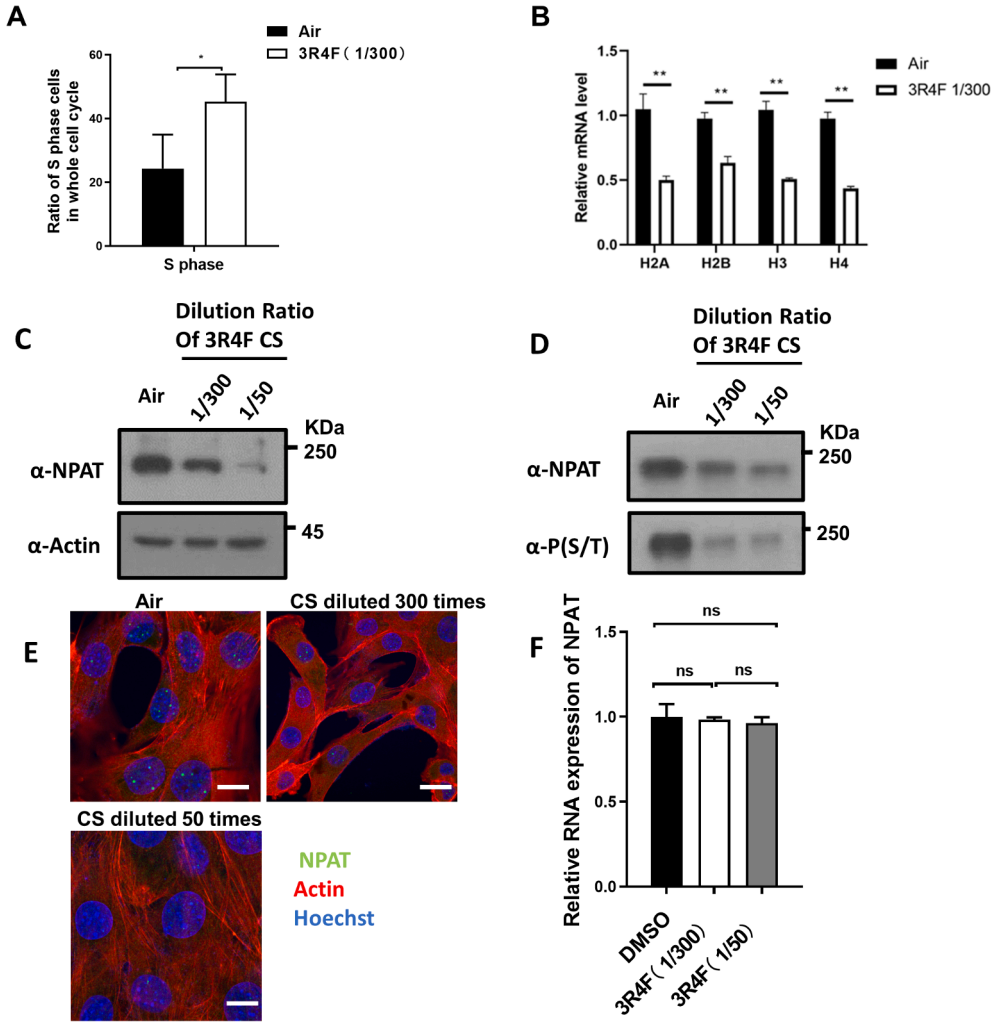

Fig. 3. CS treatment led to S phase arrest through down-regulation of NPAT. (A) FACS assay for the percentage of cells at the S phase during cell cycles in C2C12 cells treated with air or air-CS mixture (the ratio of CS and air was 1:300). Values are shown as means ± SEM. N = 3. A two-tailed unpaired Student's *t*-test was used. Significant difference from control, *p < 0.05. (B) Total mRNA of C2C12 myoblasts treated with air and air-CS mixture (the ratio of CS and air was 1:300) was extracted, and the gene expression of H2A, H2B, H3, and H4 was detected using real-time PCR. Actin was used as an internal control. Values are shown as means ± SEM. N = 3. A two-tailed unpaired Student's *t*-test was used. Significant difference from control, **p < 0.01. (C) Lysates of C2C12 myoblasts treated with air and air-CS mixture (the ratio of CS and air was 1:300 or 1:50) were western blotted with NPAT antibody. Actin antibody was used as the loading control. (D) Lysates of C2C12 myoblasts treated with air and air-CS mixture (the ratio of CS and air was 1:300 or 1:50) were immunoblotted with NPAT and p(S/T) antibody. (E) C2C12 myoblasts were treated with air and air-CS mixture (the ratio of CS and air was 1:300 or 1:50). Cell morphology of the myoblasts was observed through immunofluorescence. NPAT (green) was detected through direct staining with its antibody. Nuclei (blue) were visualized through Hoechst staining. (F) Total mRNA of C2C12 myoblasts treated with air and air-CS mixture (the ratio of CS and air was 1:300 or 1:50) was extracted, and the gene expression of NPAT was detected using real-time PCR. Actin was used as an internal control. N = 3. ANOVA followed by Dunnett's post-test was applied for comparison. Values are shown as means ± SEM. Ns: no significant. (For interpretation of the references to colour in this figure legend, the reader is referred to the web version of this article.)

3.4. CS exposure inhibited NPAT protein expression through the proteasome pathway

Our previous experiments demonstrated that smoke exposure inhibited NPAT protein expression in myoblasts without affecting their mRNA transcription. This finding suggests that CS treatment may accelerate NPAT protein degradation. We, therefore, measured the half-life of NPAT in the presence of air or CS in C2C12 myoblasts. For this, new protein synthesis was blocked by treatment with the translational inhibitor Cycloheximide (CHX). CS treatment significantly promoted the decay of endogenous NPAT (Fig. 4A). To test whether CS-triggered NPAT degradation is dependent on the ubiquitin–proteasome proteolytic pathway, we treated myoblasts with the proteasome inhibitor MG132. Notably, MG132 could restore NPAT expression levels in CS-treated myoblasts (Fig. 4B). Some studies have reported that HiNF-P can regulate the stability of NPAT protein. Increasing HiNF-P can promote the formation of the NPAT/HiNF-P complex, thereby stabilizing NPAT protein and prolonging its half-life (Miele et al., 2005). We found that CS exposure also inhibited the expression of HiNF-P (Fig. 4C). Moreover, both down-regulating of NPAT and exposure to CS could cause S phase arrest (Fig. 4D). Furthermore, pretreatment with protease inhibitor MG132 could rescue S-phase entry of myoblasts cells inhibited by CS exposure during the cell cycle (Fig. 4E). We also found overexpression of NPAT could rescue both the arrested S-phase progression and the inhibited proliferation of myoblasts cells induced by CS exposure (Fig. 4F and 4G).

4. Discussion

CS is the main cause of COPD and one of the most important risk factors for its related complications. Skeletal muscle dysfunction is a common extrapulmonary complication caused by COPD (Barreiro and Gea, 2016; Maltais et al., 2014). In COPD patients, impaired muscle function and loss of mass are common systemic findings. In these patients, breathing and limb muscles are often affected, leading to restricted breathing, poor exercise tolerance, and reduced quality of life (Coronell et al., 2004; Seymour et al., 2010). These findings support that smoke exposure is an important factor in skeletal muscle dysfunction in COPD patients. The striking observation that skeletal muscle dysfunction is likely to manifest before any significant decline in lung function has led to the concept that smoking alone may be sufficient to drive skeletal muscle dysfunction in the absence of COPD (Morse et al., 2007). Therefore, it is urgent to clarify the mechanism of muscle dysfunction induced by smoke and to search for related regulatory molecular targets to provide a new way for disease prevention and treatment.

Some studies on the effects of CS on skeletal muscle indicate that volatile and soluble components of CS, including aldehydes, reactive oxygen species, and reactive nitrogen, enter the bloodstream and reach the skeletal muscle of smokers (Rom et al., 2012). In skeletal muscle, CS components increase oxidative stress directly or through the activation of nicotinamide adenine dinucleotide phosphate (NADPH), and oxidase (NOX), and generate ROS and increase oxidative stress. CS-induced oxidative stress may lead to phosphorylation of p38 MAPK, which in turn activates the NF-kB pathway through phosphorylation of NF-kB kinase inhibitor (IKK) and NF-kB inhibitor (IkB) and proteasomal degradation of IkB, leading to nuclear translocation of NF-kB. Activated NF-kB triggers the up-regulation of muscle-specific E3 ubiquitin ligase (Meng and Yu, 2010). The up-regulation of these ligases leads to increased degradation of skeletal muscle proteins, thereby accelerating the progression of sarcopenia in smokers. However, most studies are based on mature muscle tissue or differentiated myotubes; the effect of CS exposure on skeletal muscle satellite cells and skeletal muscle regeneration is minimal. Thus, eliminating or preventing the suppressive effects of CS on skeletal muscle myoblast proliferation remains a key challenge. Our research demonstrated that smoke exposure inhibited myoblast proliferation (Fig. 1) and promoted the expression of cell cycle suppressor proteins, such as p21 and p27, and caused S phase arrest (Figs. 2 and 3).

Proliferation of myoblasts requires entry into the cell cycle for replication of genetic material. Cell cycle includes two stages: interphase (G1, S, G2) and division phase (Blagosklonny and Pardee, 2002). Cyclin-dependent kinase (CDK) and cyclin regulatory subunits are the main regulators of cell cycle. The activity of the cyclin kinase-cyclin complex in the G1 phase determines whether the cell stops dividing or enters the division cycle. This stage depends on extracellular signaling and intracellular information that leads to whether CDK can be reactivated after the previous cell cycle. After entering the cell cycle, type D cyclins (D1, D2, D3 in mammals) are expressed and CDK4 or CDK6 is activated. The RB protein is then phosphorylated, which weakens the interaction between RB and the heterodimer transcription factor E2F/DP. As a result, the inhibition of E2F by pRB is reduced, which enables the initial transcription of E2F-dependent genes, including cyclin E and other cell cycle genes. Subsequent activation of CDK2-cyclin E leads to further phosphorylation and deactivation of pRb, release of E2F, and complete entry into the S phase (Ruijtenberg and van den Heuvel, 2016). During S phase, cells begin to replicate DNA and histone proteins, which is the basis of subsequent cell division and determines whether the subsequent cell cycle can proceed smoothly. Our study confirmed that smoke exposure caused myoblasts S phase arrest by inhibiting replication dependent histone transcription (Fig. 3).

When the cell cycle is blocked by external factors or internal programmed regulation, myoblasts will exit the cell cycle. In addition to the inhibition of pRB-mediated transcription, the induced expression of some other important proteins can also reflect cell cycle exit. This includes members of two different CDK suppressor protein (CKI) families associated with CDK (Sherr and Roberts, 1999): One is the INK4 (Inhibitor of CDK4) protein family, such as p15, p16, etc., which specifically binds to CDK4/6 kinase and prevents their interaction with D-type cyclin; The other is the CIP/KIP (Cyclin-CDK-interaction protein) family, which binds to the CDK-Cyclin complex and blocks its activity. The CIP/KIP family consists of p21, p27, etc., which plays a particularly important role in the regulation of CDK2-cyclin E complex. Our research demonstrated that smoke exposure promoted the expression of both two different kinds of CKI families, such as p21, p27and p16(Fig. 2). This means that smoke exposure can affect multiple regulatory stages of the cell cycle. In the future, we can conduct more detailed studies on the regulatory mechanisms at each stage.

The cell nucleus is highly organized and contains many nuclear bodies. Even without a defining membrane, these nuclear organelles maintain structural integrity at a steady state, indicating that the mechanisms controlling nuclear body turnover differ from cytoplasmic membrane-bound organelles (Grosch et al., 2020; Sabari et al., 2020). A hierarchically ordered model and a stochastic assembly model were raised to explain how the HLB assembles (Duronio and Marzluff, 2017a). In both models, NPAT was proposed as a fundamental scaffold to recruit other components to initiate the HLB biogenesis. When cells enter the S phase, Cyclin E/CDK2-phosphorylated NPAT maintains the homeostasis of HLB, promotes the transcription of histone genes, and regulates the progression and proliferation of cells in the S phase (Duronio and Marzluff, 2017b; Ghule et al., 2018; Ling Zheng et al., 2015). In the self-renewal process of pluripotent stem cells, specific Cyclin D2 knockout can inhibit the phosphorylation of NPAT, reduce the expression of histone H4, and limit the replication of S-phase cells, suggesting that Cyclin D2-mediated phosphorylation of NPAT is an important cell cycle regulation mechanism (Becker et al., 2010; Jiang et al., 2019). This post-translational modification of NPAT is required for the association of NPAT with the histone gene promoter to initiate gene transcription. We found that CS exposure inhibited both the expression of NPAT protein and its phosphorylation regulation (Fig. 3). Besides phosphorylation, acetylation might play roles in modulating NPAT function. This was suggested by the finding that NPAT transiently interacts with CBP/p300 histone acetyltransferase and contains a potential substrate sequence for

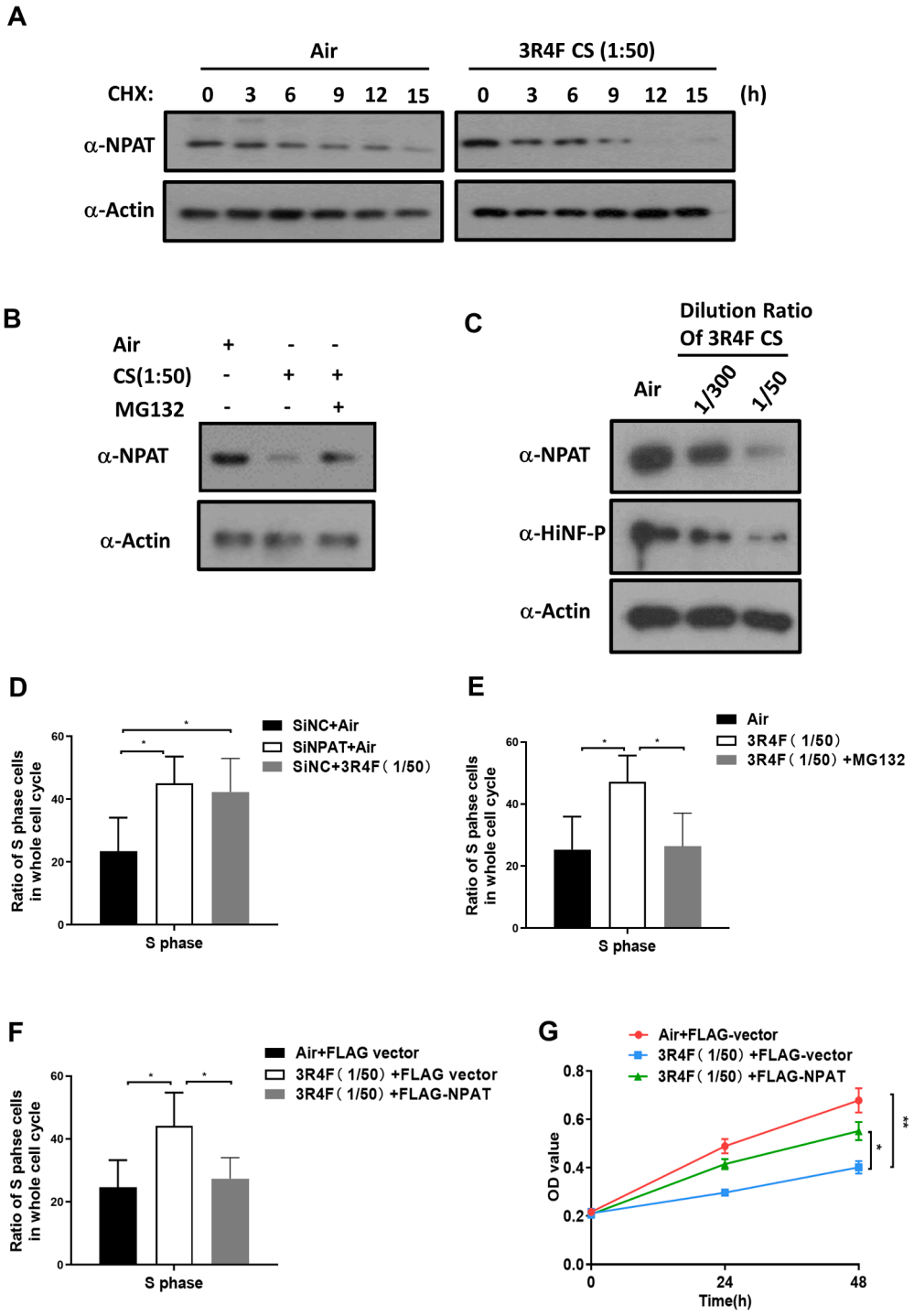

Fig. 4. CS down-regulated NPAT by promoting proteasomal degradation. (A) cycloheximide C2C12 cells were treated with (CHX) (50 μg/mL) and air or air-CS mixture (the ratio of CS and air was 1:50) for the indicated times. NPAT expression in cell lysates was tested by immunoblotting analysis. Actin antibody was used as the loading control. (B) Myoblasts were cultured with air or air-CS mixture (the ratio of CS and air was 1:50), followed by incubation with DMSO (control) or the proteasome inhibitor MG132 (4 μM) for 12 h. NPAT expression in cell lysates was tested by immunoblotting analysis. Actin antibody was used as the loading control. (C) Lysates of C2C12 myoblasts treated with air and air-CS mixture (the ratio of CS and air was 1:300 or 1:50) were immunoblotted with NPAT and HiNF-P antibody. (D) FACS assay for the percentage of cells at the S phase during cell cycles in C2C12 cells treated with air or air-CS mixture (the ratio of CS and air was 1:50), transfected with control siRNA or NPAT siRNA. Values are shown as means ± SEM. N = 3. ANOVA followed by Dunnett's post-test was applied for comparison. Significant difference from control, *$p < 0.05$. (E) FACS assay for the percentage of cells at the S phase during cell cycles in C2C12 cells treated with air or air-CS mixture (the ratio of CS and air was 1:50), followed by incubation with DMSO (control) or the proteasome inhibitor MG132 (4 μM) for 12 h. Values are shown as means ± SEM. N = 3. ANOVA followed by Dunnett's post-test was applied for comparison. Significant difference from control, *$p < 0.05$. (F) FACS assay for the percentage of cells at the S phase during cell cycles in C2C12 cells treated with air or air-CS mixture (the ratio of CS and air was 1:50) overexpressed of FLAG or FLAG-NPAT. Values are shown as means ± SEM. N = 3. ANOVA followed by Dunnett's post-test was applied for comparison. Significant difference from control, *$p < 0.05$. (G) CCK8 assay was performed on C2C12 myoblasts overexpressed of FLAG or FLAG-NPAT with or without CS (the ratio of CS and air was 1:50) treatment. Quantification analysis for OD value was performed. N = 3. ANOVA followed by Dunnett's post-test was applied for comparison. Significant difference from control, *$p < 0.05$,**$p < 0.01$.

CBP/p300 (Wang et al., 2004). In the future, we will also try to explore the regulation of smoke exposure on the acetylation level of NPAT protein. This may be another molecular mechanism that regulates myoblast proliferation.

The role of NPAT in RD histone transcription and proliferation has been extensively studied over the last decade. NPAT dysfunction contributes to cancer susceptibility. Exome sequencing reveals germline NPAT mutation as a candidate risk factor for Hodgkin lymphoma (Saarinen et al., 2011). Furthermore, NPAT variants are associated with a risk for estrogen receptor-negative breast cancer (Milne et al., 2017). Therefore, fine-tuning NPAT activation is required to ensure healthy tissue development and homeostasis. Previous works have demonstrated that the association of NPAT to FLASH, HiNF-P, YARP, and Cpn10/Hsp10 is essential for the assembly of functional HLBs (Barcaroli et al., 2006; Koreski et al., 2020; Miele et al., 2005; Zheng et al., 2015). Interestingly, no evidence shows that NPAT could directly bind to the histone gene promoter, although it played critical roles in activating histone gene transcription. This was explained by the finding that NPAT links directly to a histone nuclear factor, HiNF-P. Down-regulation of HiNF-P reduces the association of NPAT with the histone H4 promoter and impairs its transcription (Miele et al., 2005). Further study has revealed that exogenous expression of HiNF-P enhances the stabilization of NPAT. We found that CS exposure induced NPAT degradation in C2C12 myoblasts and impaired myogenic proliferation through HiNF-P-associated proteasomal-dependent mechanisms. As an application of the proteasome inhibitor MG132 or overexpression of NPAT could reverse CS-induced impairments in myoblast proliferation (Figs. 3 and 4). Given the broad tissue expression pattern of NPAT, its regulatory mechanism may play a role in divergent aspects of tissue development and regeneration.

Studies of the adverse effects induced by CS mainly focused on examing the release of some toxic substances in CS. However, CS is an extremely complex and dynamic compound. So chemical composition analysis can't fully characterize the possible harm of CS to the human body. So, in vitro air–liquid interface models of respiratory tract tissue have been improved to assess the toxicity and cellular response of cigarette smoke. Our study is based on the use of Borgwaldt RM20S to produce CS-explored cells. In our experiment, reference cigarette 3R4F was introduced in the system. 3R4F reference cigarette is a 'US style' blended product (University of Kentucky), The tar content is 9.4 mg/cig and the nicotine content is 0.73 mg/cig (Crooks et al., 2013). Earlier our partner team reported the development of an algorithm based on quantitative assessment of transcriptomic profiles and signaling pathway perturbation analysis (SPPA) of human bronchial epithelial cells (HBEC) exposed to the toxic components present in CS using the same machine. HBEC were exposed to CS of different compositions and for different durations using an ISO3308 smoking regime and the impact of exposure was monitored in 2263 signaling pathways in the cell to generate a total effect score that reflects the quantitative degree of impact of external stimuli on the cells(Chen et al., 2021).Considering the fact that the concentration of smoke inhaled and the concentration of toxic substances in the blood cannot be controlled when people smoke, a set of instruments that can produce relatively stable and repeatable smoke concentrations is particularly important. By experiments *in vitro*, our finding has therefore shed light on CS-induced muscle dysfunction and raised the possibility that the ubiquitin–proteasome proteolytic pathway of NPAT protein could be a potential therapeutic target.

CRediT authorship contribution statement

Jianfeng Wang: Writing - original draft, Investigation. **Jinling Liu:** Conceptualization. **Jingjing Shao:** Formal analysis. **Hongyu Chen:** Resources. **Luyun Cui:** Investigation. **Pei Zhang:** Data curation. **Yinan Yao:** Methodology. **Jianying Zhou:** Funding acquisition, Validation. **Zhang Bao:** Writing - review & editing, Supervision.

Funding

This study was supported by a Project from the Department of Science and Technology of Zhejiang Province (2019C03042) and the medical and health research project of Zhejiang province (2021KY156).

Declaration of competing interest

The authors declare that they have no known competing financial interests or personal relationships that could have appeared to influence the work reported in this paper.

Data availability

The data that has been used is confidential.

Appendix A. Supplementary data

Supplementary data to this article can be found online at https://doi.org/10.1016/j.crtox.2024.100161.

References

Agusti, A., Celli, B.R., Criner, G.J., Halpin, D., Anzueto, A., Barnes, P., Bourbeau, J., Han, M.K., Martinez, F.J., Montes de Oca, M., Mortimer, K., Papi, A., Pavord, I., Roche, N., Salvi, S., Sin, D.D., Singh, D., Stockley, R., Lopez Varela, M.V., Wedzicha, J.A., Vogelmeier, C.F., 2023. Global initiative for chronic obstructive lung disease 2023 report: GOLD executive summary. Eur. Respir. J. 61.

Barcaroli, D., Bongiorno-Borbone, L., Terrinoni, A., Hofmann, T.G., Rossi, M., Knight, R. A., Matera, A.G., Melino, G., De Laurenzi, V., 2006. FLASH is required for histone transcription and S-phase progression. PNAS 103, 14808–14812.

Barreiro, E., Gea, J., 2016. Molecular and biological pathways of skeletal muscle dysfunction in chronic obstructive pulmonary disease. Chron. Respir. Dis. 13, 297–311.

Becker, K.A., Ghule, P.N., Lian, J.B., Stein, J.L., van Wijnen, A.J., Stein, G.S., 2010. Cyclin D2 and the CDK substrate p220(NPAT) are required for self-renewal of human embryonic stem cells. J. Cell. Physiol. 222, 456–464.

Blagosklonny, M.V., Pardee, A.B., 2002. The restriction point of the cell cycle. Cell Cycle 1, 103–110.

Castillo, E.M., Goodman-Gruen, D., Kritz-Silverstein, D., Morton, D.J., Wingard, D.L., Barrett-Connor, E., 2003. Sarcopenia in elderly men and women: The Rancho Bernardo study. Am. J. Prev. Med. 25, 226–231.

Chen, H., Chen, X., Shen, Y., Yin, X., Liu, F., Liu, L., Yao, J., Chu, Q., Wang, Y., Qi, H., Timko, M.P., Fang, W., Fan, L., 2021. Signaling pathway perturbation analysis for assessment of biological impact of cigarette smoke on lung cells. Sci. Rep. 11, 16715.

Christenson, S.A., Smith, B.M., Bafadhel, M., Putcha, N., 2022. Chronic obstructive pulmonary disease. Lancet 399, 2227–2242.

Cong, X.X., Gao, X.K., Rao, X.S., Wen, J., Liu, X.C., Shi, Y.P., He, M.Y., Shen, W.L., Shen, Y., Ouyang, H., Hu, P., Low, B.C., Meng, Z.X., Ke, Y.H., Zheng, M.Z., Lu, L.R., Liang, Y.H., Zheng, L.L., Zhou, Y.T., 2020. Rab5a activates IRS1 to coordinate IGF-AKT-mTOR signaling and myoblast differentiation during muscle regeneration. Cell Death Differ.

Coronell, C., Orozco-Levi, M., Mendez, R., Ramirez-Sarmiento, A., Galdiz, J.B., Gea, J., 2004. Relevance of assessing quadriceps endurance in patients with COPD. Eur. Respir. J. 24, 129–136.

Crooks, I., Dillon, D.M., Scott, J.K., Ballantyne, M., Meredith, C., 2013. The effect of long term storage on tobacco smoke particulate matter in in vitro genotoxicity and cytotoxicity assays. Regul. Toxicol. Pharm. 65, 196–200.

Dumont, N.A., Bentzinger, C.F., Sincennes, M.C., Rudnicki, M.A., 2015. Satellite cells and skeletal muscle regeneration. Compr. Physiol. 5, 1027–1059.

Duronio, R.J., Marzluff, W.F., 2017. Coordinating cell cycle-regulated histone gene expression through assembly and function of the histone locus body. RNA Biol. 14, 726–738.

Ghule, P.N., Seward, D.J., Fritz, A.J., Boyd, J.R., van Wijnen, A.J., Lian, J.B., Stein, J.L., Stein, G.S., 2018. Higher order genomic organization and regulatory compartmentalization for cell cycle control at the G1/S-phase transition. J. Cell. Physiol. 233, 6406–6413.

Grosch, M., Ittermann, S., Shaposhnikov, D., Drukker, M., 2020. Chromatin-associated membraneless organelles in regulation of cellular differentiation. Stem Cell Rep. 15, 1220–1232.

Hood, D.A., Memme, J.M., Oliveira, A.N., Triolo, M., 2019. Maintenance of skeletal muscle mitochondria in health, exercise, and aging. Annu. Rev. Physiol. 81, 19–41.

Ito, A., Hashimoto, M., Tanihata, J., Matsubayashi, S., Sasaki, R., Fujimoto, S., Kawamoto, H., Hosaka, Y., Ichikawa, A., Kadota, T., Fujita, Y., Takekoshi, D., Ito, S., Minagawa, S., Numata, T., Hara, H., Matsuoka, T., Udaka, J., Araya, J., Saito, M., Kuwano, K., 2022. Involvement of Parkin-mediated mitophagy in the pathogenesis of chronic obstructive pulmonary disease-related sarcopenia. J. Cachexia. Sarcopenia Muscle 13, 1864–1882.

Jiang, X., Yin, S., Fan, S., Bao, J., Jiao, Y., Ali, A., Iqal, F., Xu, J., Zhang, Y., Shi, Q., 2019. Npat-dependent programmed Sertoli cell proliferation is indispensable for testis cord development and germ cell mitotic arrest. FASEB J. 33, 9075–9086.
Kaczmarek, A., Kaczmarek, M., Cialowicz, M., Clemente, F.M., Wolanski, P., Badicu, G., Murawska-Cialowicz, E., 2021. The role of satellite cells in skeletal muscle regeneration-the effect of exercise and age. Biology (Basel) 10.
Karimian, A., Ahmadi, Y., Yousefi, B., 2016. Multiple functions of p21 in cell cycle, apoptosis and transcriptional regulation after DNA damage. DNA Repair (Amst) 42, 63–71.
Kim, S.Y., Lee, J.H., Huh, J.W., Ro, J.Y., Oh, Y.M., Lee, S.D., An, S., Lee, Y.S., 2011. Cigarette smoke induces Akt protein degradation by the ubiquitin-proteasome system. J. Biol. Chem. 286, 31932–31943.
Koreski, K.P., Rieder, L.E., McLain, L.M., Chaubal, A., Marzluff, W.F., Duronio, R.J., 2020. Drosophila histone locus body assembly and function involves multiple interactions. Mol. Biol. Cell 31, 1525–1537.
Lee, J.S., Auyeung, T.W., Kwok, T., Lau, E.M., Leung, P.C., Woo, J., 2007. Associated factors and health impact of sarcopenia in older chinese men and women: a cross-sectional study. Gerontology 53, 404–410.
Lee, K.H., Woo, J., Kim, J., Lee, C.H., Yoo, C.G., 2021. Cigarette smoke extract decreased basal and lipopolysaccharide-induced expression of MARCO via degradation of p300. Respirology 26, 102–111.
Ling Zheng, L., Wang, F.Y., Cong, X.X., Shen, Y., Rao, X.S., Huang, D.S., Fan, W., Yi, P., Wang, X.B., Zheng, L., Zhou, Y.T., Luo, Y., 2015. Interaction of heat shock protein Cpn10 with the cyclin E/Cdk2 substrate nuclear protein ataxia-telangiectasia (NPAT) is involved in regulating histone transcription. J. Biol. Chem. 290, 29290–29300.
Maltais, F., Decramer, M., Casaburi, R., Barreiro, E., Burelle, Y., Debigare, R., Dekhuijzen, P.N., Franssen, F., Gayan-Ramirez, G., Gea, J., Gosker, H.R., Gosselink, R., Hayot, M., Hussain, S.N., Janssens, W., Polkey, M.I., Roca, J., Saey, D., Schols, A.M., Spruit, M.A., Steiner, M., Taivassalo, T., Troosters, T., Vogiatzis, I., Wagner, P.D., COPD, A.E.A.H.C.o.L.M.D.i., 2014. An official American Thoracic Society/European Respiratory Society statement: update on limb muscle dysfunction in chronic obstructive pulmonary disease. Am. J. Respir. Crit. Care Med. 189, e15–e62.
Mao, Y.S., Zhang, B., Spector, D.L., 2011. Biogenesis and function of nuclear bodies. Trends Genet. 27, 295–306.
Mendiratta, S., Gatto, A., Almouzni, G., 2019. Histone supply: Multitiered regulation ensures chromatin dynamics throughout the cell cycle. J. Cell Biol. 218, 39–54.
Meng, S.J., Yu, L.J., 2010. Oxidative stress, molecular inflammation and sarcopenia. Int. J. Mol. Sci. 11, 1509–1526.
Miele, A., Braastad, C.D., Holmes, W.F., Mitra, P., Medina, R., Xie, R., Zaidi, S.K., Ye, X., Wei, Y., Harper, J.W., van Wijnen, A.J., Stein, J.L., Stein, G.S., 2005. HiNF-P directly links the cyclin E/CDK2/p220NPAT pathway to histone H4 gene regulation at the G1/S phase cell cycle transition. Mol. Cell Biol. 25, 6140–6153.
Milne, R.L., Kuchenbaecker, K.B., Michailidou, K., Beesley, J., Kar, S., Lindstrom, S., Hui, S., Lemacon, A., Soucy, P., Dennis, J., Jiang, X., Rostamianfar, A., Finucane, H., Bolla, M.K., McGuffog, L., Wang, Q., Aalfs, C.M., Investigators, A., Adams, M., Adlard, J., Agata, S., Ahmed, S., Ahsan, H., Aittomaki, K., Al-Ejeh, F., Allen, J., Ambrosone, C.B., Amos, C.I., Andrulis, I.L., Anton-Culver, H., Antonenkova, N.N., Arndt, V., Arnold, N., Aronson, K.J., Auber, B., Auer, P.L., Ausems, M., Azzollini, J., Bacot, F., Balmana, J., Barile, M., Barjhoux, L., Barkardottir, R.B., Barrdahl, M., Barnes, D., Barrowdale, D., Baynes, C., Beckmann, M.W., Benitez, J., Bermisheva, M., Bernstein, L., Bignon, Y.J., Blazer, K.R., Blok, M.J., Blomqvist, C., Blot, W., Bobolis, K., Boeckx, B., Bogdanova, N.V., Bojesen, A., Bojesen, S.E., Bonanni, B., Borresen-Dale, A.L., Bozsik, A., Bradbury, A.R., Brand, J.S., Brauch, H., Brenner, H., Bressac-de Paillerets, B., Brewer, C., Brinton, L., Broberg, P., Brooks-Wilson, A., Brunet, J., Bruning, T., Burwinkel, B., Buys, S.S., Byun, J., Cai, Q., Caldes, T., Caligo, M.A., Campbell, I., Canzian, F., Caron, O., Carracedo, A., Carter, B.D., Castelao, J.E., Castera, L., Caux-Moncoutier, V., Chan, S.B., Chang-Claude, J., Chanock, S.J., Chen, X., Cheng, T.D., Chiquette, J., Christiansen, H., Claes, K.B.M., Clarke, C.L., Conner, T., Conroy, D.M., Cook, J., Cordina-Duverger, E., Cornelissen, S., Coupier, I., Cox, A., Cox, D.G., Cross, S.S., Cuk, K., Cunningham, J. M., Czene, K., Daly, M.B., Damiola, F., Darabi, H., Davidson, R., De Leeneer, K., Devilee, P., Dicks, E., Diez, O., Ding, Y.C., Ditsch, N., Doheny, K.F., Domchek, S.M., Dorfling, C.M., Dork, T., Dos-Santos-Silva, I., Dubois, S., Dugue, P.A., Dumont, M., Dunning, A.M., Durcan, L., Dwek, M., Dworniczak, B., Eccles, D., Eeles, R., Ehrencrona, H., Eilber, U., Ejlertsen, B., Ekici, A.B., Eliassen, A.H., Embrace, Engel, C., Eriksson, M., Fachal, L., Faivre, L., Fasching, P.A., Faust, U., Figueroa, J., Flesch-Janys, D., Fletcher, O., Flyger, H., Foulkes, W.D., Friedman, E., Fritschi, L., Frost, D., Gabrielson, M., Gaddam, P., Gammon, M.D., Ganz, P.A., Gapstur, S.M., Garber, J., Garcia-Barberan, V., Garcia-Saenz, J.A., Gaudet, M.M., Gauthier-Villars, M., Gehrig, A., Collaborators, G.S., Georgoulias, V., Gerdes, A.M., Giles, G.G., Glendon, G., Godwin, A.K., Goldberg, M.S., Goldgar, D.E., Gonzalez-Neira, A., Goodfellow, P., Greene, M.H., Alnaes, G.I.G., Grip, M., Gronwald, J., Grundy, A., Gschwantler-Kaulich, D., Guenel, P., Guo, Q., Haeberle, L., Hahnen, E., Haiman, C. A., Hakansson, N., Hallberg, E., Hamann, U., Hamel, N., Hankinson, S., Hansen, T.V. O., Harrington, P., Hart, S.N., Hartikainen, J.M., Healey, C.S., Hebon, Hein, A., Helbig, S., Henderson, A., Heyworth, J., Hicks, B., Hillemanns, P., Hodgson, S., Hogervorst, F.B., Hollestelle, A., Hooning, M.J., Hoover, B., Hopper, J.L., Hu, C., Huang, G., Hulick, P.J., Humphreys, K., Hunter, D.J., Imyanitov, E.N., Isaacs, C., Iwasaki, M., Izatt, L., Jakubowska, A., James, P., Janavicius, R., Janni, W., Jensen, U. B., John, E.M., Johnson, N., Jones, K., Jones, M., Jukkola-Vuorinen, A., Kaaks, R., Kabisch, M., Kaczmarek, K., Kang, D., Kast, K., kConFab, A.I., Keeman, R., Kerin, M. J., Kets, C.M., Keupers, M., Khan, S., Khusnutdinova, E., Kiiski, J.I., Kim, S.W., Knight, J.A., Konstantopoulou, I., Kosma, V.M., Kristensen, V.N., Kruse, T.A., Kwong, A., Laenkholm, A.V., Laitman, Y., Lalloo, F., Lambrechts, D., Landsman, K., Lasset, C., Lazaro, C., Le Marchand, L., Lecarpentier, J., Lee, A., Lee, E., Lee, J.W., Lee, M.H., Lejbkowicz, F., Lesueur, F., Li, J., Lilyquist, J., Lincoln, A., Lindblom, A., Lissowska, J., Lo, W.Y., Loibl, S., Long, J., Loud, J.T., Lubinski, J., Luccarini, C., Lush, M., MacInnis, R.J., Maishman, T., Makalic, E., Kostovska, I.M., Malone, K.E., Manoukian, S., Manson, J.E., Margolin, S., Martens, J.W.M., Martinez, M.E., Matsuo, K., Mavroudis, D., Mazoyer, S., McLean, C., Meijers-Heijboer, H., Menendez, P., Meyer, J., Miao, H., Miller, A., Miller, N., Mitchell, G., Montagna, M., Muir, K., Mulligan, A.M., Mulot, C., Nadesan, S., Nathanson, K.L., Collaborators, N., Neuhausen, S.L., Nevanlinna, H., Nevelsteen, I., Niederacher, D., Nielsen, S.F., Nordestgaard, B.G., Norman, A., Nussbaum, R.L., Olah, E., Olopade, O.I., Olson, J.E., Olswold, C., Ong, K.R., Oosterwijk, J.C., Orr, N., Osorio, A., Pankratz, V.S., Papi, L., Park-Simon, T.W., Paulsson-Karlsson, Y., Lloyd, R., Pedersen, I.S., Peissel, B., Peixoto, A., Perez, J.I.A., Peterlongo, P., Peto, J., Pfeiler, G., Phelan, C.M., Pinchev, M., Plaseska-Karanfilska, D., Poppe, B., Porteous, M.E., Prentice, R., Presneau, N., Prokofieva, D., Pugh, E., Pujana, M.A., Pylkas, K., Rack, B., Radice, P., Rahman, N., Rantala, J., Rappaport-Fuerhauser, C., Rennert, G., Rennert, H.S., Rhenius, V., Rhiem, K., Richardson, A., Rodriguez, G.C., Romero, A., Romm, J., Rookus, M.A., Rudolph, A., Ruediger, T., Saloustros, E., Sanders, J., Sandler, D.P., Sangrajrang, S., Sawyer, E.J., Schmidt, D.F., Schoemaker, M.J., Schumacher, F., Schurmann, P., Schwentner, L., Scott, C., Scott, R.J., Seal, S., Senter, L., Seynaeve, C., Shah, M., Sharma, P., Shen, C.Y., Sheng, X., Shimelis, H., Shrubsole, M.J., Shu, X.O., Side, L.E., Singer, C.F., Sohn, C., Southey, M.C., Spinelli, J.J., Spurdle, A.B., Stegmaier, C., Stoppa-Lyonnet, D., Sukiennicki, G., Surowy, H., Sutter, C., Swerdlow, A., Szabo, C.I., Tamimi, R.M., Tan, Y.Y., Taylor, J.A., Tejada, M.I., Tengstrom, M., Teo, S.H., Terry, M.B., Tessier, D.C., Teule, A., Thone, K., Thull, D.L., Tibiletti, M.G., Tihomirova, L., Tischkowitz, M., Toland, A.E., Tollenaar, R., Tomlinson, I., Tong, L., Torres, D., Tranchant, M., Truong, T., Tucker, K., Tung, N., Tyrer, J., Ulmer, H.U., Vachon, C., van Asperen, C.J., Van Den Berg, D., van den Ouweland, A.M.W., van Rensburg, E.J., Varesco, L., Varon-Mateeva, R., Vega, A., Viel, A., Vijai, J., Vincent, D., Vollenweider, J., Walker, L., Wang, Z., Wang-Gohrke, S., Wappenschmidt, B., Weinberg, C.R., Weitzel, J.N., Wendt, C., Wesseling, J., Whittemore, A.S., Wijnen, J.T., Willett, W., Winqvist, R., Wolk, A., Wu, A.H., Xia, L., Yang, X.R., Yannoukakos, D., Zaffaroni, D., Zheng, W., Zhu, B., Ziogas, A., Ziv, E., Zorn, K.K., Gago-Dominguez, M., Mannermaa, A., Olsson, H., Teixeira, M.R., Stone, J., Offit, K., Ottini, L., Park, S.K., Thomassen, M., Hall, P., Meindl, A., Schmutzler, R.K., Droit, A., Bader, G.D., Pharoah, P.D.P., Couch, F.J., Easton, D.F., Kraft, P., Chenevix-Trench, G., Garcia-Closas, M., Schmidt, M.K., Antoniou, A.C., Simard, J., 2017. Identification of ten variants associated with risk of estrogen-receptor-negative breast cancer. Nat. Genet. 49, 1767–1778.
Morse, D., Rosas, I.O., 2014. Tobacco smoke-induced lung fibrosis and emphysema. Annu. Rev. Physiol. 76, 493–513.
Morse, C.I., Wust, R.C., Jones, D.A., de Haan, A., Degens, H., 2007. Muscle fatigue resistance during stimulated contractions is reduced in young male smokers. Acta Physiol. (Oxf.) 191, 123–129.
Nizami, Z., Deryusheva, S., Gall, J.G., 2010a. The Cajal body and histone locus body. Cold Spring Harb. Perspect. Biol. 2, a000653.
Nizami, Z.F., Deryusheva, S., Gall, J.G., 2010b. Cajal bodies and histone locus bodies in drosophila and xenopus. Cold Spring Harb. Symp. Quant. Biol. 75, 313–320.
Rom, O., Kaisari, S., Aizenbud, D., Reznick, A.Z., 2012. Identification of possible cigarette smoke constituents responsible for muscle catabolism. J. Muscle Res. Cell Motil. 33, 199–208.
Ruijtenberg, S., van den Heuvel, S., 2016. Coordinating cell proliferation and differentiation: Antagonism between cell cycle regulators and cell type-specific gene expression. Cell Cycle 15, 196–212.
Saarinen, S., Aavikko, M., Aittomaki, K., Launonen, V., Lehtonen, R., Franssila, K., Lehtonen, H.J., Kaasinen, E., Broderick, P., Tarkkanen, J., Bain, B.J., Bauduer, F., Unal, A., Swerdlow, A.J., Cooke, R., Makinen, M.J., Houlston, R., Vahteristo, P., Aaltonen, L.A., 2011. Exome sequencing reveals germline NPAT mutation as a candidate risk factor for Hodgkin lymphoma. Blood 118, 493–498.
Sabari, B.R., Dall'Agnese, A., Young, R.A., 2020. Biomolecular condensates in the nucleus. Trends Biochem. Sci. 45, 961–977.
Seymour, J.M., Spruit, M.A., Hopkinson, N.S., Natanek, S.A., Man, W.D., Jackson, A., Gosker, H.R., Schols, A.M., Moxham, J., Polkey, M.I., Wouters, E.F., 2010. The prevalence of quadriceps weakness in COPD and the relationship with disease severity. Eur. Respir. J. 36, 81–88.
Sherr, C.J., Roberts, J.M., 1999. CDK inhibitors: positive and negative regulators of G1-phase progression. Genes Dev. 13, 1501–1512.
Sleeman, J.E., Trinkle-Mulcahy, L., 2014. Nuclear bodies: new insights into assembly/dynamics and disease relevance. Curr. Opin. Cell Biol. 28, 76–83.
Stampfli, M.R., Anderson, G.P., 2009. How cigarette smoke skews immune responses to promote infection, lung disease and cancer. Nat. Rev. Immunol. 9, 377–384.
Szulc, P., Duboeuf, F., Marchand, F., Delmas, P.D., 2004. Hormonal and lifestyle determinants of appendicular skeletal muscle mass in men: the MINOS study. Am. J. Clin. Nutr. 80, 496–503.
Wang, A., Ikura, T., Eto, K., Ota, M.S., 2004. Dynamic interaction of p220(NPAT) and CBP/p300 promotes S-phase entry. Biochem. Biophys. Res. Commun. 325, 1509–1516.
Wright, D.J., Day, F.R., Kerrison, N.D., Zink, F., Cardona, A., Sulem, P., Thompson, D.J., Sigurjonsdottir, S., Gudbjartsson, D.F., Helgason, A., Chapman, J.R., Jackson, S.P., Langenberg, C., Wareham, N.J., Scott, R.A., Thorsteindottir, U., Ong, K.K., Stefansson, K., Perry, J.R.B., 2017. Genetic variants associated with mosaic Y chromosome loss highlight cell cycle genes and overlap with cancer susceptibility. Nat. Genet. 49, 674–679.

Ye, X., Wei, Y., Nalepa, G., Harper, J.W., 2003. The cyclin E/Cdk2 substrate p220(NPAT) is required for S-phase entry, histone gene expression, and Cajal body maintenance in human somatic cells. Mol. Cell Biol. 23, 8586–8600.
Zhang, J., Zhao, J., Dahan, P., Lu, V., Zhang, C., Li, H., Teitell, M.A., 2018. Metabolism in pluripotent stem cells and early mammalian development. Cell Metab. 27, 332–338.
Zheng, L.L., Wang, F.Y., Cong, X.X., Shen, Y., Rao, X.S., Huang, D.S., Fan, W., Yi, P., Wang, X.B., Zheng, L., Zhou, Y.T., Luo, Y., 2015. Interaction of heat shock protein Cpn10 with the cyclin E/Cdk2 substrate nuclear protein ataxia-telangiectasia (NPAT) is involved in regulating histone transcription. J. Biol. Chem. 290, 29290–29300.